Active slivering of oceanic crust along the Molucca ridge (Indonesia-Philippine): Implication for ophiolite incorporation in a subduction wedge?

Anne-Gaëlle Bader, Manuel Pubellier, Claude Rangin, Christine Deplus, Rémy Louat

TECTONICS, VOL. 18, NO. 4, PAGES 606-620, AUGUST 1999

Active slivering of oceanic crust along the Molucca ridge (Indonesia-Philippine): Implication for ophiolite incorporation in a subduction wedge?

Anne Gaëlle Bader,[1] Manuel Pubellier, and Claude Rangin
Laboratoire de Géologie de l'Ecole Normale Supérieure, Paris

Christine Deplus and Rémy Louat[2]
Institut de Physique du Globe, Paris

Abstract. A recent marine geophysical survey in the northern Molucca Sea revealed the structure to be that of a classical active convergent margin. We observe from west to east a volcanic arc (Sangihe), a forearc basin resting on an outer ridge (the Molucca ridge), which serves as a buttress for an accretionary wedge, and a composite downgoing plate (Snellius Ridge and Philippine Sea Basin). Gravity modeling indicates a strong negative anomaly above the wedge, which cannot be explained with reasonable density values. Modeling imposes a basement deepening and a rupture of the 700-km-long subducting lithosphere. This process individualized the lithospheric slab from the Snellius Ridge, which in turn was separated recently from the south Philippine Basin by the incipient Philippine Trench. This induces a deformation of the forearc region with backthrusting of the outer ridge and forearc basin, visible on bathymetry and seismic data. We extrapolate the tectonic emplacement of such oceanic blocks to the Oligocene times in order to explain the origin of the Pujada Miangas outer ridge as a sliver previously incorporated to the margin, and we discuss the possibility of this deformation process being fabric for terrane accretion.

1. Introduction

The Molucca Sea is a narrow basin in which oceanic crust is only known indirectly and is supposed to have almost completely disappeared by subduction. It is located south of Mindanao (Philippines), at the junction between three major converging plates: Eurasian, Australian, and Philippine Sea plate (Figure 1, insert). The east thinned edge of the Eurasian plate is bounded by an active volcanic arc: the Sangihe arc, extending from the northern arm of Sulawesi to southwest of Mindanao (Sarangani Peninsula). Only the southern part of this arc (from Sulawesi to Sangihe island) is still active. In the south of the Molucca Sea (from 0°N to 3°30'N), the Molucca basin has been subducting eastward beneath Halmahera since the Pliocene [*Nichols et al.*, 1990; *Hall et al.*, 1991]. More recent datings would extend this arc activity to the late Miocene [*Hall et al.*, 1995].

Dismembered ophiolites crop out in a chain of islands which occupies a narrow strip bisecting the Molucca Sea. The largest outcrops are found in the Talaud islands, but smaller occurrences have also been reported in Tifore island [*Moore et al.*, 1980; *Evans et al.*, 1983; *Sukamto and Suwarna*, 1986]. These islands are underlain by a series of discontinuous ridges which presently occupy the central part of the Molucca Sea (Figure 1). These ridges are called the Molucca ridge and comprise the Mayu Ridge in the south Molucca Sea, the Talaud Ridge, and the Pujada Ridge (PR) and Miangas Ridges (MR) to the north. In the south Molucca Sea the ultramafics exposed in the Mayu and Tifore islands have been interpreted as the emergence of a sliver of the Molucca oceanic crust broken at the apex of the double-verging subduction and incorporated in the collision complex [*Silver and Moore*, 1978, 1981; *Hamilton*, 1979; *McCaffrey et al.*, 1980]. The tectonic setting of these ophiolites is therefore interpreted as the result of this arc-arc collision.

The MODEC cruise of R/V. L'Atalante [*Rangin et al.*, 1996] revealed a very distinct tectonic setting in the northern Molucca Sea. The PR and MR extending south into Talaud island are also made of ophiolites exposed in Talaud island and the Pujada peninsula [*Silver and Moore*, 1978, 1981; *Pubellier et al.*, 1991a, 1996; *Quebral et al.*, 1996]. These new bathymetric and seismic reflection data revealed that the Miangas Ridge (MR in Figures 1 and 7) is actually the outer ridge of the Sangihe subduction zone [*Rangin et al.*, 1996]. In Talaud the Miocene forearc arc sediments onlap the ultramafic basement of the ridge, meaning they were emplaced during middle Tertiary, prior to the recent arc-arc collision [*Evans et al.*, 1983].

In order to resolve the issue of the origin of the ultramafic ridge (broken Molucca Sea crust versus outer ridge of the Sangihe subduction zone), we have compiled the geological and gravity data available along the ridge [*Silver and Moore*, 1978; *McCaffrey et al.*, 1980; *McCaffrey*, 1982, 1991]. We compared these data with bathymetry, seismic, and ocean bottom seismometer (OBS) data collected along the northern part of the ridge during the MODEC cruise. More generally, this paper questions the origin of oceanic crustal fragments present in the accretionary wedges of subduction zones. Are they part of a process of incorporation of oceanic crust slivers during subduction, or do they result from microblock accretion, like the ophiolitic suture present in many mountain belts?

2. Central Molucca Sea Model Revisited

Refraction profiles of *McCaffrey et al.* [1980] reveal that the central part of the Molucca basin is composed of around 15 km of thick heterogeneous material (the collision complex), which induces a large, negative free air anomaly (down to -230 mGal

[1] Now at Institut Français du Pétrole, Rueil Malmaison
[2] Also at Institut de Recherche pour le Développement, UR6, Paris

Paper number 1999TC900004.
0278-7407/99/1999TC900004$12.00

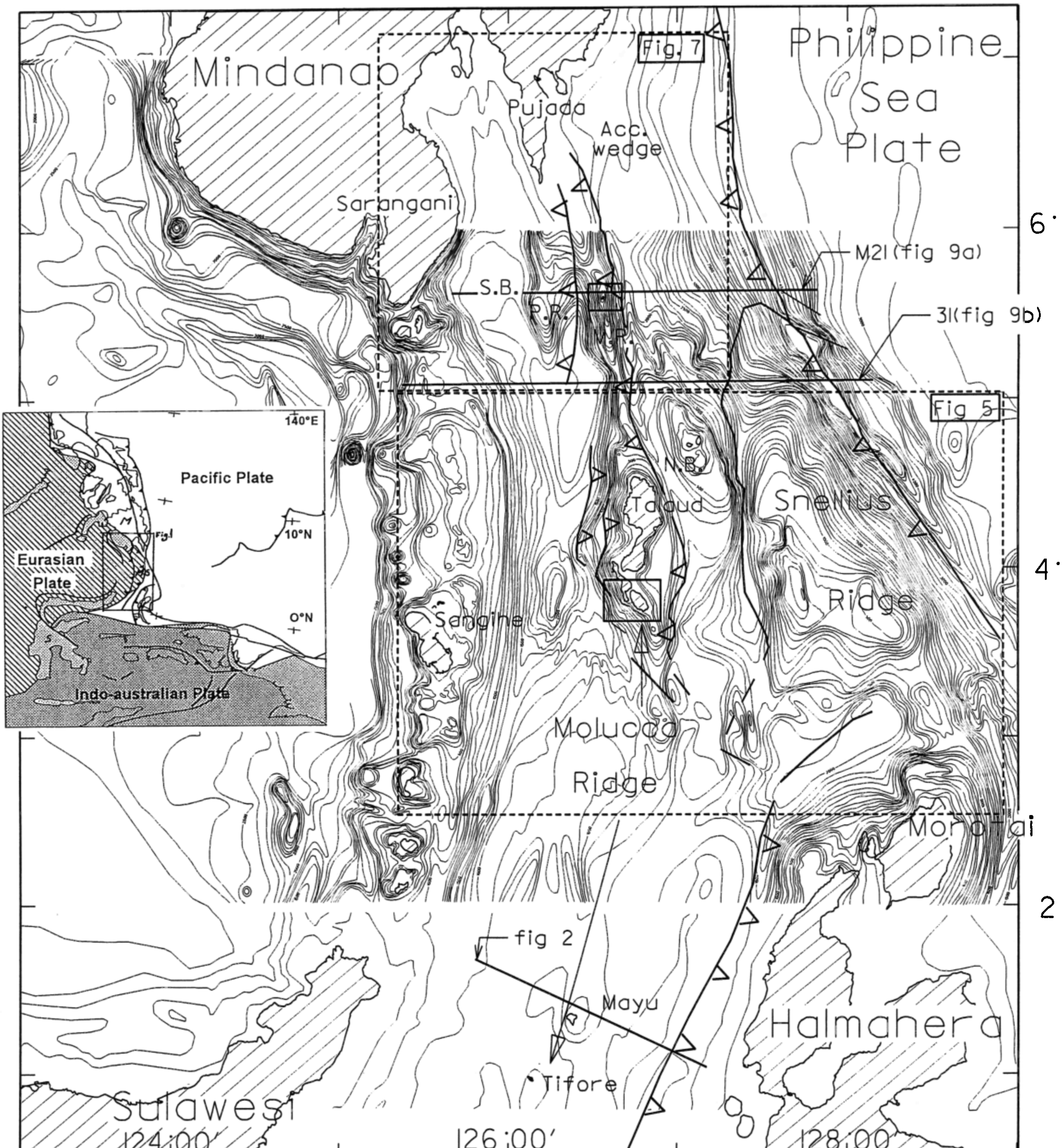

Figure 1. Bathymetric map of the Molucca Sea from Krause [1966]. Isobaths are every 100 feet. In the area not covered by the Krause data, bathymetry from the General Bathymetric Chart of the Oceans (GEBCO) database (isobaths every 500 m). The domains will be described in the paper. Solid lines show emplacement of two-dimentional (2-D) gravity modeling (Figure 2, 9a, and 9b). The dashed boxes outline the emplacement of Figures 5 and 7. Solid box show the area covered by the northern ocean bottom seismometer (OBS) network. SB, Sangihe Basin; PR, Pujada Ridge; MTR, Mayu-Talaud Ridge; NB Nanusa Bank. The insert is a map showing the three major plates in the MODEC cruise area. M, Mindanao; S, Sulawesi; H, Halmahera; MS, Molucca Sea.

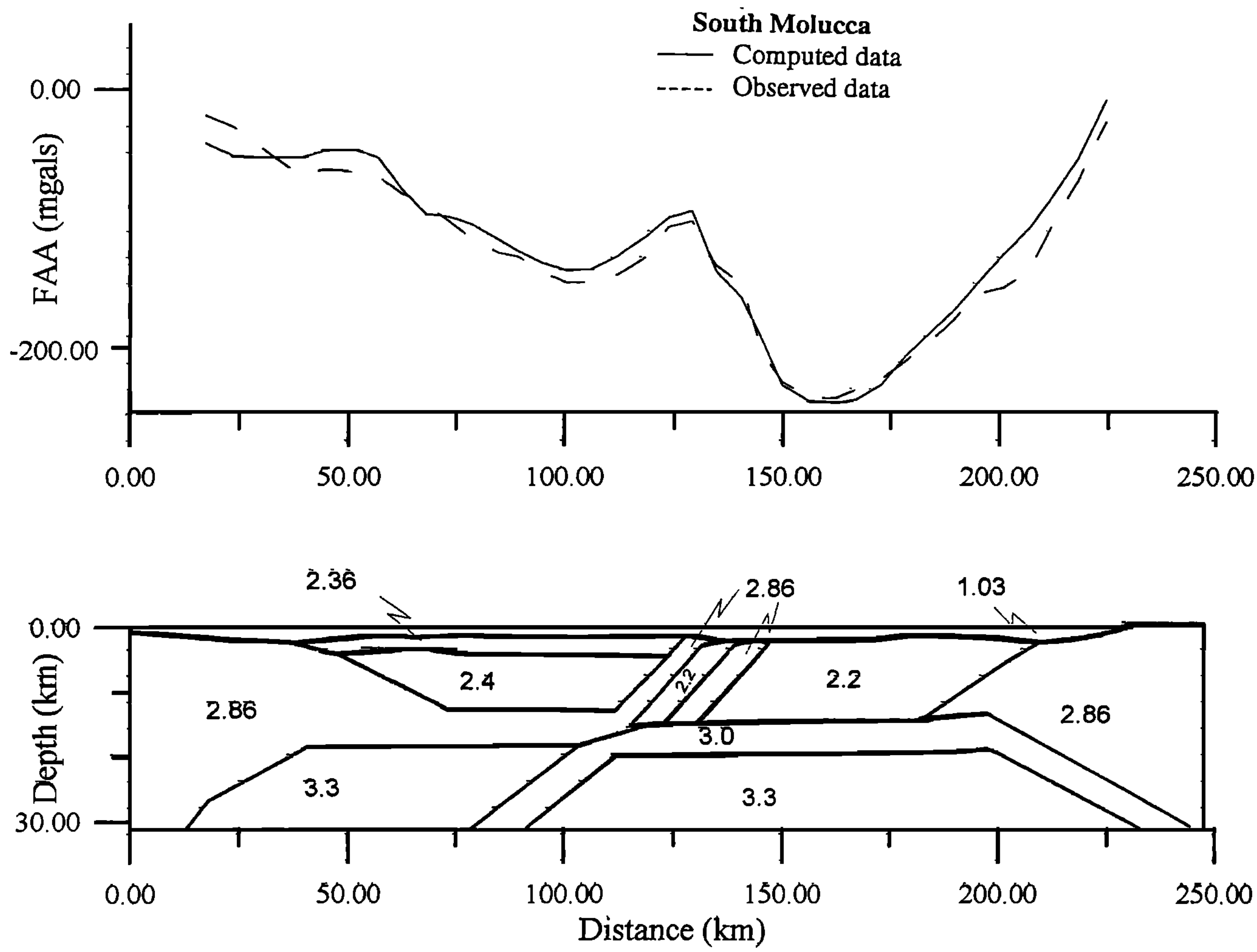

Figure 2. Gravity model located in the southern part of the Molucca Sea basin, north of Mayu island. Gravity data and thickness of the bodies are from *McCaffrey et al.* [1980]. See location on Figures 1 and 4. FAA, free air anomaly.

north of Mayu island). Although reflection data are not good enough within the collision complex, refraction profiles show that the basement is several kilometers shallower to the west of the ridge than it is to the east. This observation, as well as the asymmetric shape of the regional free air anomaly over the basin, suggests the existence of a fault beneath the Mayu-Tifore Ridge [*McCaffrey et al.*, 1980].

McCaffrey et al. [1980] showed that the top of the ridge is marked by a local high in the gravity field (50 mGal above the average regional anomaly). This high is explained by the density of peridotite and gabbro exposed in the Mayu and Talaud islands, and it would indicate the presence of a piece of oceanic crust, thrusted over the collision complex.

In order to integrated it into the discussion and to compare it with the northern Molucca Sea, we have computed the gravity data presented by *McCaffrey et al.* [1980]. The refraction data used by these authors were also used to constrain the thickness of the different bodies. The residual anomaly calculated for one of these previous models [*McCaffrey et al.*, 1980, Figure 12] (not illustrated) shows a small narrow peak (70 mGal) on the eastern slope of the ridge and a broad moderate misfit along the wedge (20 mGal).

When we applied on the same profile the densities used for the northern Molucca Sea, meaning a forearc basin to the west of the Mayu-Tifore Ridge and a lighter accretionary wedge to the east, a good fit is obtained on the wedge (Figure 2). The difference of density between these two sedimentary bodies (the forearc basin and the wedge) may as well explain the asymmetric shape of the negative free air anomaly over the basin. Actually, the hypothesis of a nonsymmetrical lithologies model better fits with values around 2.2 for the wedge and 2.4 for the forearc basin.

The positive peak, centered over the ridge, is constrained by the ophiolitic nature of the ridge. In our model, we have introduced a second slice of high-density material. One sliver represents the top of the Mayu-Tifore Ridge, and the second one, not visible in the bathymetry, is located east of the ridge, in the accretionary wedge. This change overcomes the problem of the ridge misfit. This double-ridged model is supported by our observations on the Pujada-Miangas Ridge which is developed below. However, the link between the Mayu-Tifore and the Pujada-Miangas Ridges remains speculative at this stage. Furthermore, in our model, the ridge represents the backstop of the Sangihe subduction (Figure 2). This model imposes that the subducting slab descends westward into the mantle starting from

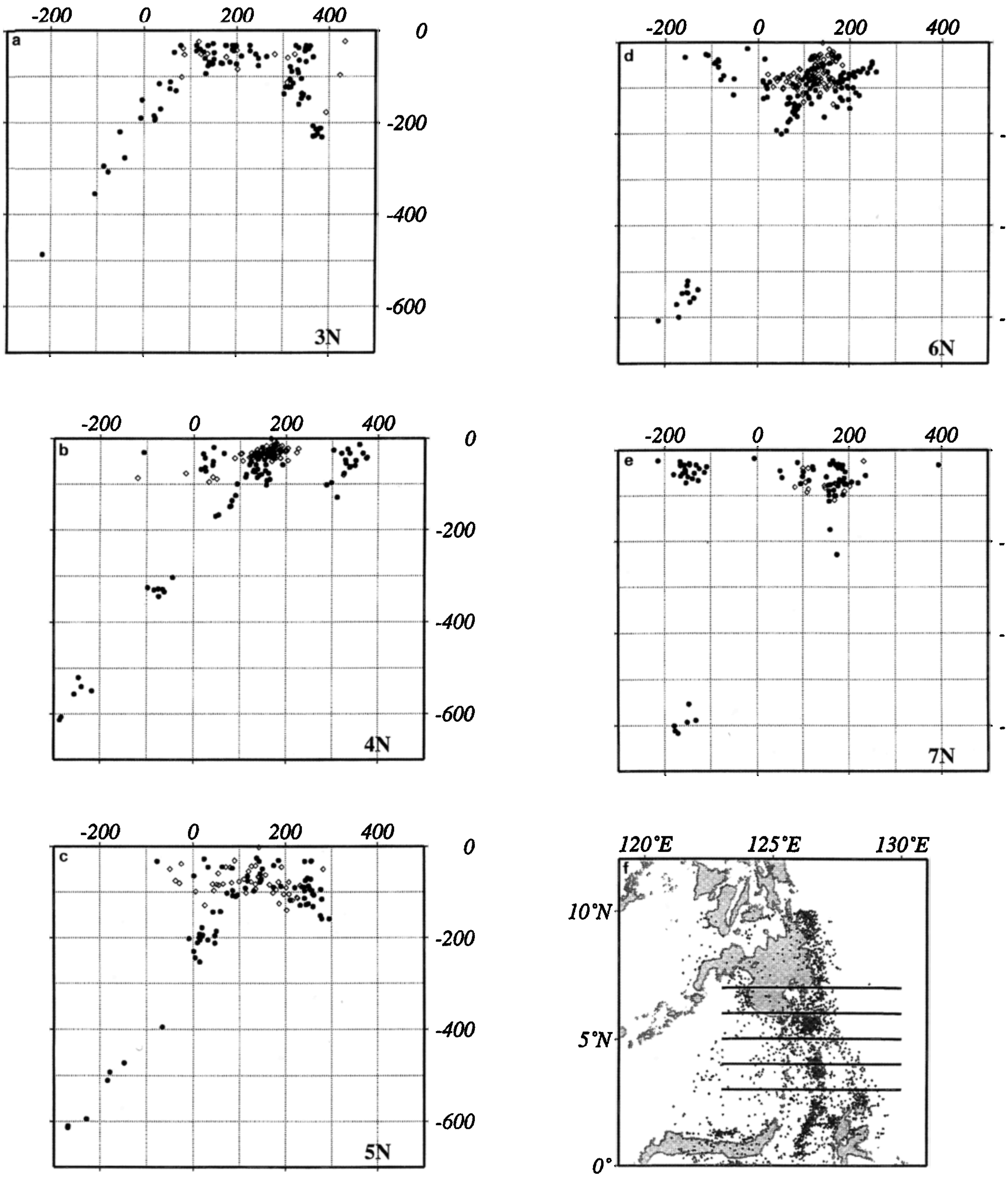

Figure 3. Seismicity profiles located at (a) 3°; (b) 4°; (c) 5°; (d) 6° and (e) 7°N. (f) location of the seismicity profiles. Each profile includes events 30' north and south of the track 0 corresponding to longitude 125°E. Horizontal and vertical scales are in kilometers.
Solid circles indicate global seismicity (from preliminary determination of epicenters (PDE) catalog). Diamonds indicate microseismicity recorded during the MODEC cruise by the two networks of OBS.

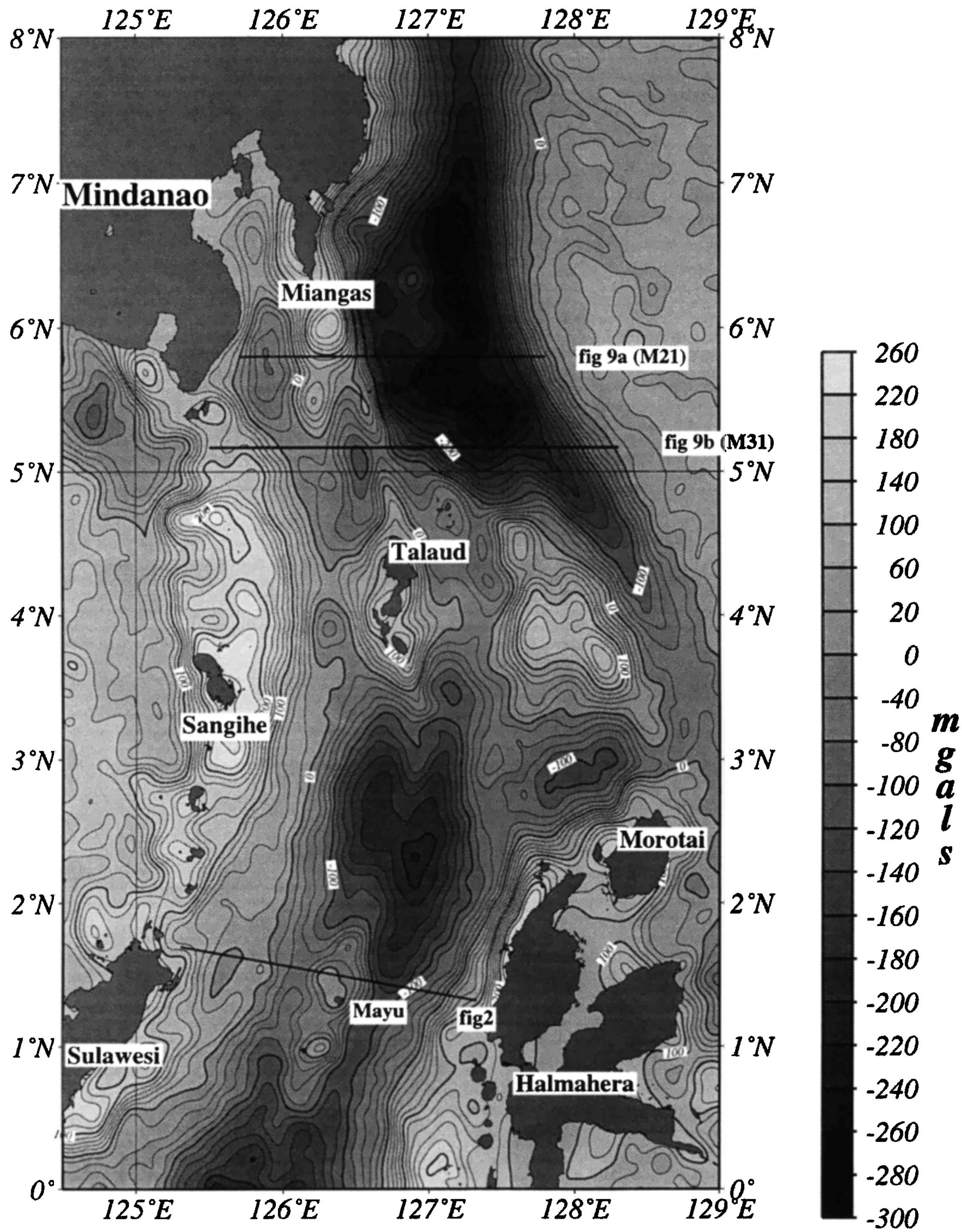

Figure 4. Free air gravity anomaly map from *Smith and Sandwell* [1995] database. Isogals are every 25 mGal. Solid lines show the location of the 2-D gravity modeling presented in Figures 2, 9a and 9b.

this point. This is in agreement with global seismicity as well as with OBS results (R. Louat, personal communication, 1997).

Serial sections of seismicity (including global seismicity and OBS recording seismicity) are illustrated in Figure 6. Each profile, located every 1° from 3°N (Figure 3a) to 7°N (Figure 3e) includes events 30' north and south of the track line. The east dipping Halmahera lithosphere, clearly present on the 3°N section, disappears northward, meaning that it is not present or seismically active. On tomographic sections (not illustrated), a cold east dipping lithosphere is present as north as 7°N (W. Spakmann, personal communication, 1996). For this reason we favor the presence of the Halmahera slab as far as the northern

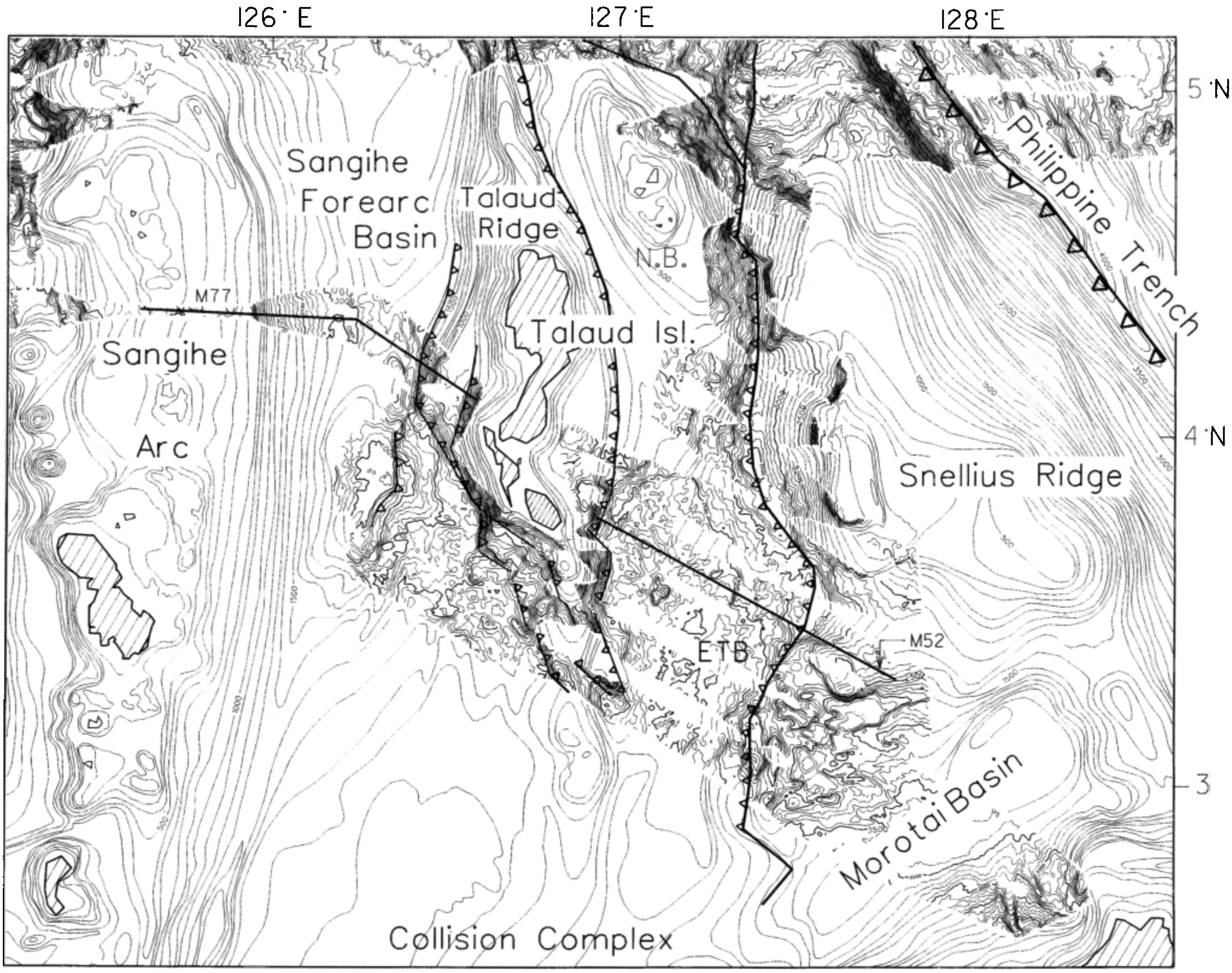

Figure 5. Bathymetric map obtained during the MODEC cruise in the area of the Talaud islands. Bold lines show the locations of the seismic lines of Figure 6a and 6b. ETB, east Talaud Bank.

Molucca sea. However, this inactive slab would be presently detached from the actual collision zone.

Contrarily, the west dipping Sangihe lithosphere can be seen from south to north of the Molucca Sea. The profiles were centered on 125°E (corresponding to track 0 on the sections). The slab is projected to the surface at 200 km east of the central line and just above the Molucca Ridge. This way, the west dipping Beniof zone appears to be steeper and seismically disrupted northward; meanwhile, shallow seismicity increases. This may be an indicator of increasing coupling between the upper and lower plates toward the north [*Huang et al.*, 1997].

The transition between the south Molucca Sea and the northern part of the basin is also marked in the gravity and bathymetry. The positive gravity anomaly above the ridge is disrupted by an important free air gravity low [*Smith and Sandwell*, 1995] between 2° and 3°N (Figure 4). At this latitude (south of the Talaud island) the sharp ridge morphology around the Talaud islands becomes a large and smooth bulge.

3. Geophysical Data Above the Molucca Ridge and Vicinity

The MODEC cruise results shed light on the overall structure in the northern Molucca Sea (from 3°N to Mindanao). These data show that the Sangihe arc and trough represent an arc forearc system which was shortened in the north by east-verging thrusts [*Rangin et al.*, 1996]. The correlation of the Miocene and Pliocene series suggests an extension of this arc system into southwest Mindanao [*Pubellier et al.*, 1991a, 1996]. Gravity data, as well as land geology in Talaud island, already showed the ophiolitic nature of the outer ridge, but little was known about the submarine morphology.

3.1. Talaud Ridge

The Talaud Ridge (Figure 5) extends from 3°N to the north where it connects with the Miangas Ridge (Figure 1). Its southern

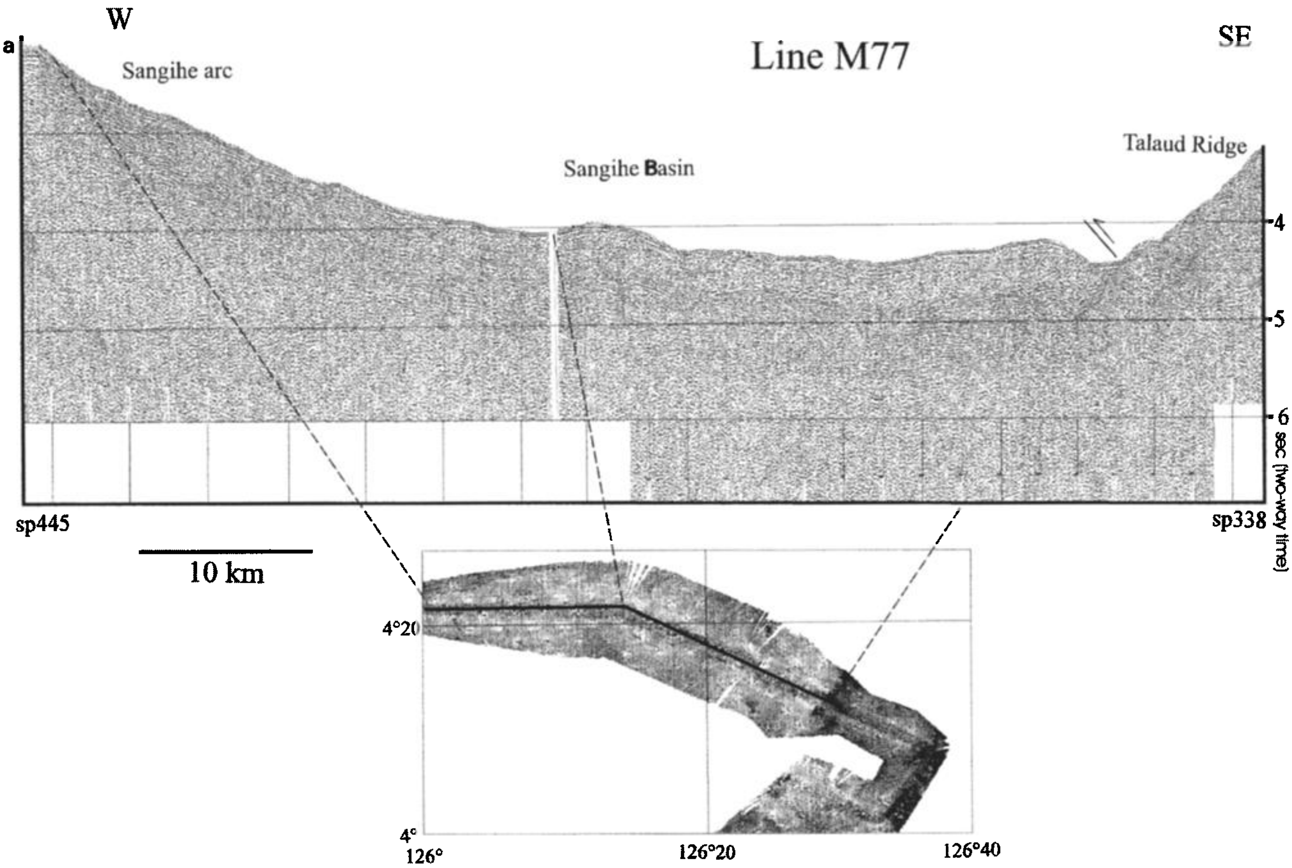

Figure 6. Seismic lines around Talaud island. See location in Figure 5 (lines M77 and M52) and on Figure 7 (line M25). (a) Line M77, the slightly deformed forearc basin (Sangihe Basin). The inset shows the reflectivity data. The major part of the shortening is accommodated along the NW-SE thrusts of the Talaud Ridge on the basin. (b) The contact between the Snellius Ridge and the wedge. The top of the Snellius ridge can be followed under the wedge. (c) The contact between the Pujada Ridge, the Miangas Ridge and the Sangihe forearc basin in front of the Sarangani Peninsula.

edge is marked by a series of parallel cliffs which trend approximately 150°N. These features were interpreted as left-lateral strike-slip faults. They control the coastline of the two southern islands of the Talaud group and the trend of folds and reverse faults located on the main island. These faults are also marked by steep gradients on the free air gravity map (Figure 4).

3.2. West Talaud Bank

Conventional 6 channel seismic lines (Figure 6) show that the west Talaud Bank of *Rangin et al.* [1996] (Figure 5) is actually a part of the Sangihe forearc basin locally shortened by the E-W shortening indicated by seismic data (Figure 6a). We observed that the eastern and western flanks of the ridge are controlled by reverse faults (Figures 5, 6a and 6b). The ridge overthrusts the east Talaud Bank to the east and is also brought onto the forearc by an east dipping reverse fault to the west (Figure 6a). Folds and active reverse faults are also visible on reflectivity data. They affect the mud line immediately west of Talaud island with west verging thrusts on lines M25 (Figure 6c) and M77 (Figure 6a). To the north the deformed zone widens again and opens toward the Sangihe forearc basin.

3.3. East Talaud Bank

The East Talaud bank of *Rangin et al.* [1996] corresponds to the collision complex of *Silver and Moore* [1978]. We hereafter refer to this unit as the accretionary wedge of the Sangihe arc because of the style of deformation and the low-density sedimentary nature. It is an area of varying width which is flat SE of Talaud and 3 s two-way time thick, with an irregular surface. It narrows northward to become a north-south trending trough between 4°N and 4°40'N. Its eastern flank is bounded by a low-angle thrust (Figure 6b), which brings it onto the Snellius Ridge [*Silver and Moore*, 1978]. Northward, the east Talaud Bank disappears under the ridge and connects with the Nanusa bank, which is a prominent unit of the accretionary wedge of unknown nature. North of the Nanusa Bank the wedge widens again and is a large dome which extends as far as Mindanao (Figure 7).

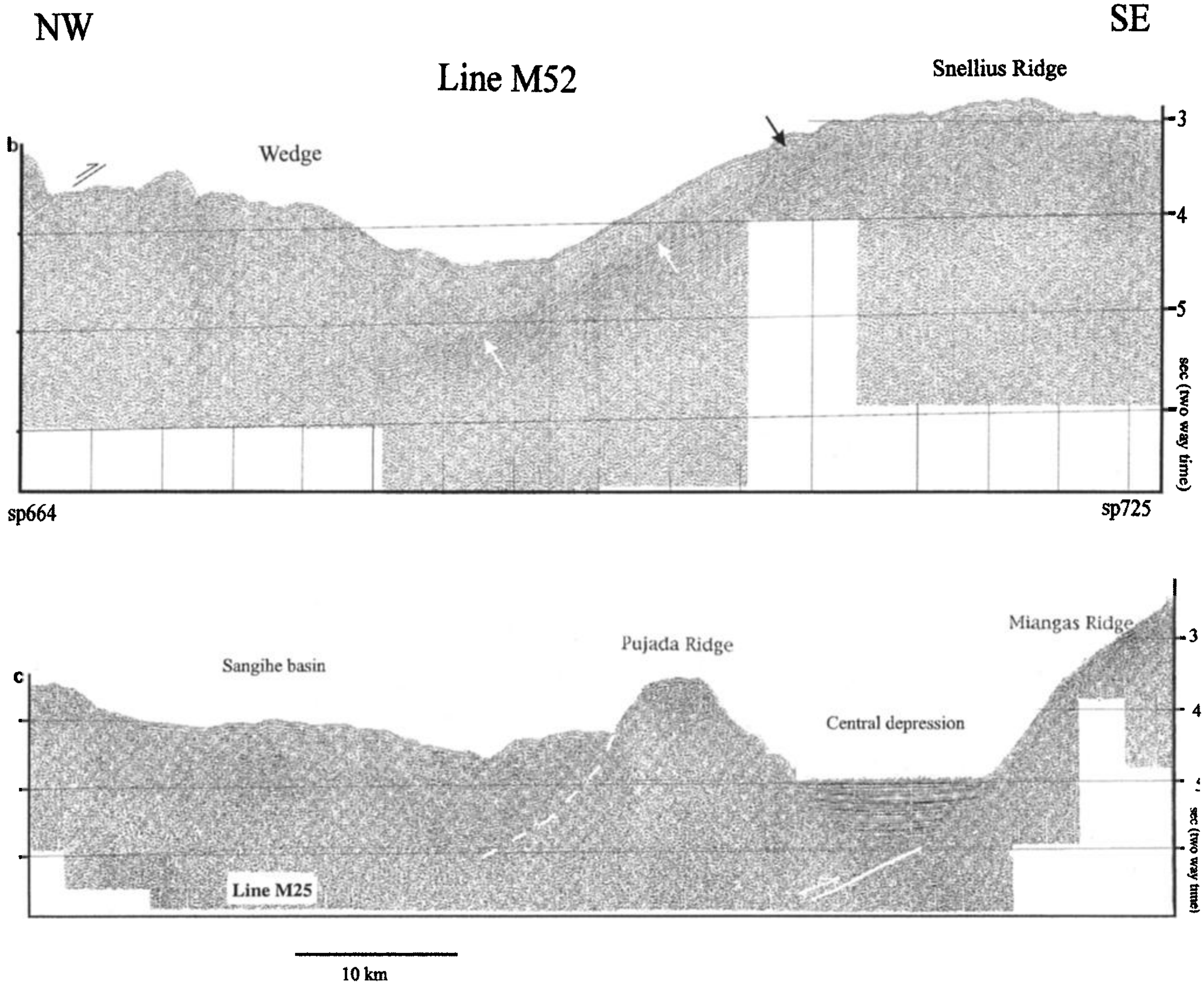

Figure 6. (Continued)

3.4. The Snellius Ridge

The Snellius Ridge is a large monocline dipping regularly to the west. It may be traced beneath the east Talaud and Nanusa Banks. It is capped by well-developed reflectors that may image a platform limestone. The plateau is underlined by a positive gravity anomaly indicative of a dense crust compatible with an ophiolitic or arc volcanic basement (Figure 4).

The southern edge of the Snellius Ridge is overthrusted by the Morotai Basin, a 70°N elongated trough separating the Snellius Ridge from the Morotai islands. The Snellius Ridge therefore disappears beneath the Morotai Basin and the accretionary wedge (Figure 6b). The bathymetric texture of the Snellius Ridge resembles that of the inner wall of the trench east of Mindanao. It is therefore suspected that the plateau represents the continuity between Halmahera and eastern Mindanao.

North of 5°, the north-south high, which bisects the basin, is composed of two separate ridges: the eastern Miangas Ridge (MR in Figure 7), which crops out at the Miangas islands, and the western Pujada Ridge (PR in Figure 7). These two ridges connect northward to the Pujada peninsula (Figures 7 and 8).

3.5. Miangas Ridge

The Miangas Ridge represents the along-strike extension of the Talaud Ridge. It trends broadly 160°N, but accurate bathymetry shows it to be composed of 00°N segments offset by 140°N sinistral strike-slip faults (Figure 7). The top of the ridge culminates at 1700 meters below seafloor (mbsf) and is marked by a strong gravity positive anomaly. The ridge crops out on the Miangas island. There, on the eastern part of the island, volcanic rocks have been described (Miangas Volcanics) [*Sukamto and Suwarna*, 1986] composed of breccia, tuff, and lava. Stratifically, they are equivalent to the Awit Formation described on the Talaud islands (middle Miocene) and thus are coeval with the inferred onset of the Sangihe arc. This unit is also exposed on the Nanusa islands [*Sukamto and Suwarna*, 1986].

The eastern flank of the ridge reveals a steep bathymetric and gravity gradient (more than 15 mGal/km). Eastward, a negative free air anomaly (-300 mGal) is induced by the presence of a thick unit of low-density material (Figure 7). This unit is strongly deformed by thrusts, folds, and landslides. We interpret this unit as the proper accretionary wedge of the Sangihe subduction zone,

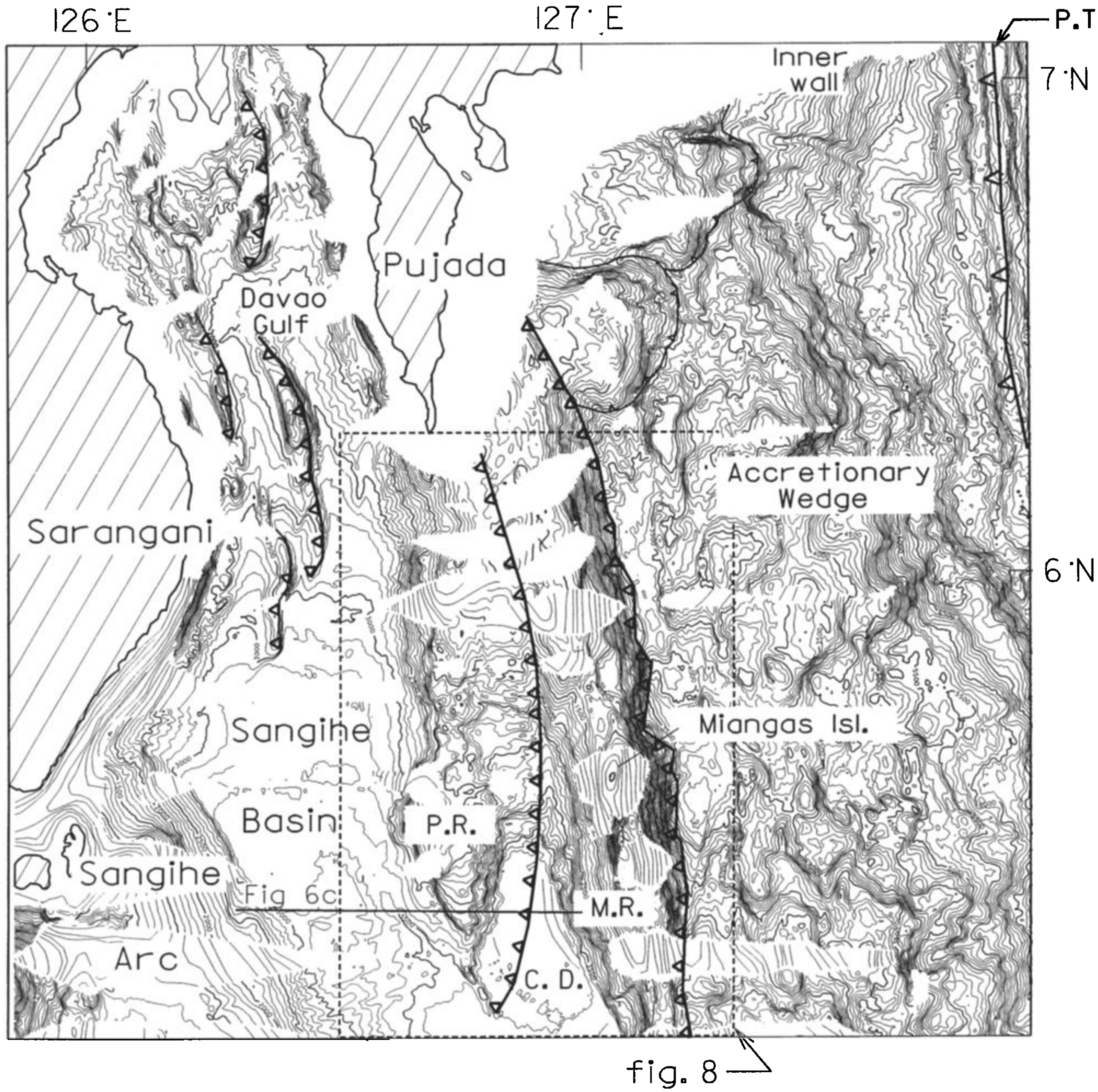

Figure 7. Bathymetric map obtained during the MODEC cruise in the area of Miangas island. Solid line shows line M25 from Figure 6c. CD, central depression; PT, Philippine Trench.

jammed under a high-density backstop: the Pujada and Miangas Ridges. This interpretation is supported by seismicity data obtained by an OBS network deployed around the Miangas island during the MODEC cruise as well as the global seismicity data from the preliminary determination of epicenters (PDE) (Figure 3). These data showed the presence of a west dipping thrust plane below the ridge. This thrust cannot be observed on the seismic profiles owing to the dense ridge with high seismic velocity, but one can assume its emergence in the basins located at the foot of the ridge (Figures 7 and 8).

The west dipping strong reflectors of the western flank of the Miangas Ridge plunge beneath an undeformed basin. The basin (the central depression) is filled with 1 to 2 s two-way time of sediments and slopes gently to the south (Figure 6c), suggesting clastic feeding from the north. The clastic deposits partly obscure a major thrust of the western Pujada Ridge over the Miangas Ridge, which crops out in the Pujada peninsula [*Hawkins et al.*, 1985; *Quebral et al.*, 1996]. Because there is apparently not enough topography to make a source for the clastics, we propose that the clastics originate from the erosion of the thrust.

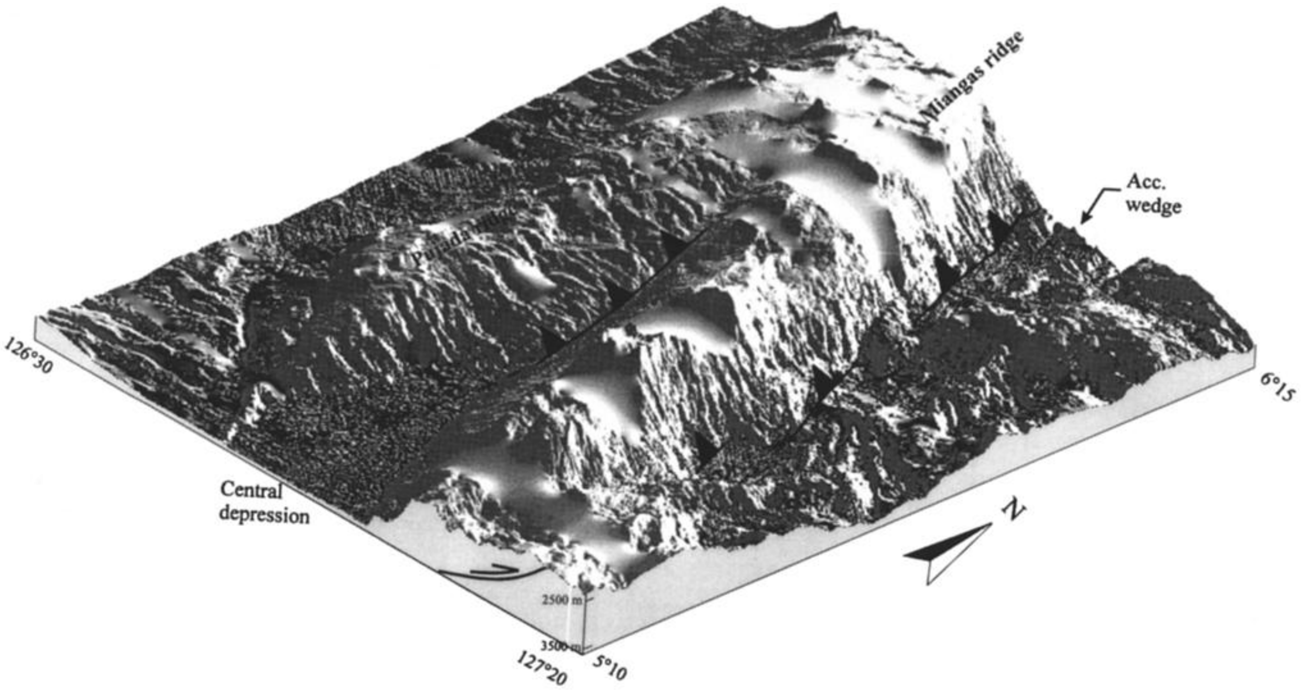

Figure 8. Digital terrane model of the southern part of the composite Pujada-Miangas Ridge. Visualization is to the NW. Lightening is from the north. Bold lines indicate the emergence of the thrusts of the Pujada Ridge on the Miangas Ridge and of the Miangas Ridge on the accretionary wedge. Smooth area indicates data gap.

3.6. Pujada Ridge

The Pujada Ridge is also a north-south high. Its crest descends slowly to the south and disappears at 5°N. The ridge seems truncated to the south by a 150°N escarpment.

To the north, both the Pujada and Miangas Ridges converge into the Pujada peninsula. The peninsula exposes dominantly ultramafic rocks including peridotites, gabbros, and basalts, with a back arc geochemical signature associated with metavolcanics and metasediments [*Hawkins et al.*, 1985]. The map of the southern part of the peninsula shows two ophiolitic bodies thrusted onto a series of metavolcanics.

Westward, the Sangihe Basin onlaps the back of the Pujada Ridge (Figure 6c). This basin was interpreted as a forearc shortened to the north in the Davao Gulf.

4. Gravity Data and Modeling

4.1. Gravity Map

A free air anomaly (FAA) map was processed after the MODEC cruise [*Rangin et al.*, 1996] and was completed with the Sandwell gravity data [*Smith and Sandwell*, 1995] (Figure 4).

In the southern part of the Molucca Sea the gravity field reaches -200 mGal. This negative FAA does not fit well with the bathymetry, and we assume the influence of the basement structure. Furthermore, the low FAA is exposed along a N-S trend situated east of the basin axis. This was interpreted by *McCaffrey et al.* [1980] as the result of a basement deepening to the east. This also causes the FAA gradient to be steeper along the coast of Halmahera (11 mGal/km versus 4.5 mGal/km along the Sangihe arc). Furthermore, the Sangihe arc induces a strong, narrow positive anomaly (up to +200 mGal at 3°30'N) whereas the gravimetric signature of the Halmahera shelf, flatter and more moderate, resembles the one of the Snellius Ridge.

North of 3°30'N, the FAA map is significantly different. On the western part of the basin the gravity anomalies are well correlated with the bathymetry. The Sangihe slope is characterized by a regular gradient. The lower values are centered on the highly sedimented Sangihe forearc. The Talaud islands and the Snellius Ridge are underlined by a positive anomaly separated by a low corresponding to the Nanusa trough.

From the Talaud islands up to Mindanao the continuous gravity high (+160 mGal) fits closely with the bathymetric high (the double Pujada-Miangas Ridge) and indicates the presence of dense bodies constituting the Molucca Ridge. These dense bodies could indicate an ophiolitic basement related to the submarine extension of the Pujada peninsula where ophiolites have been described on land [*Hawkins et al.*, 1985; *Quebral et al.*, 1996].

East of the ridge, the pattern of the gravity anomalies is rather unusual as it does not reflect the bathymetric features. An important FAA gravity low (-300 mGal) is centered over the lower slope of the accretionary wedge, 20 km west of the trench axis. This gravity low cannot be explained by the topography of the trench and thus corresponds to an important low-density body beneath the slope. Furthermore, between the ridge and this low a steep gradient of about 10 mGal/km is linear with a NNW-SSE direction and runs over the location of the southern extension of the Philippine fault.

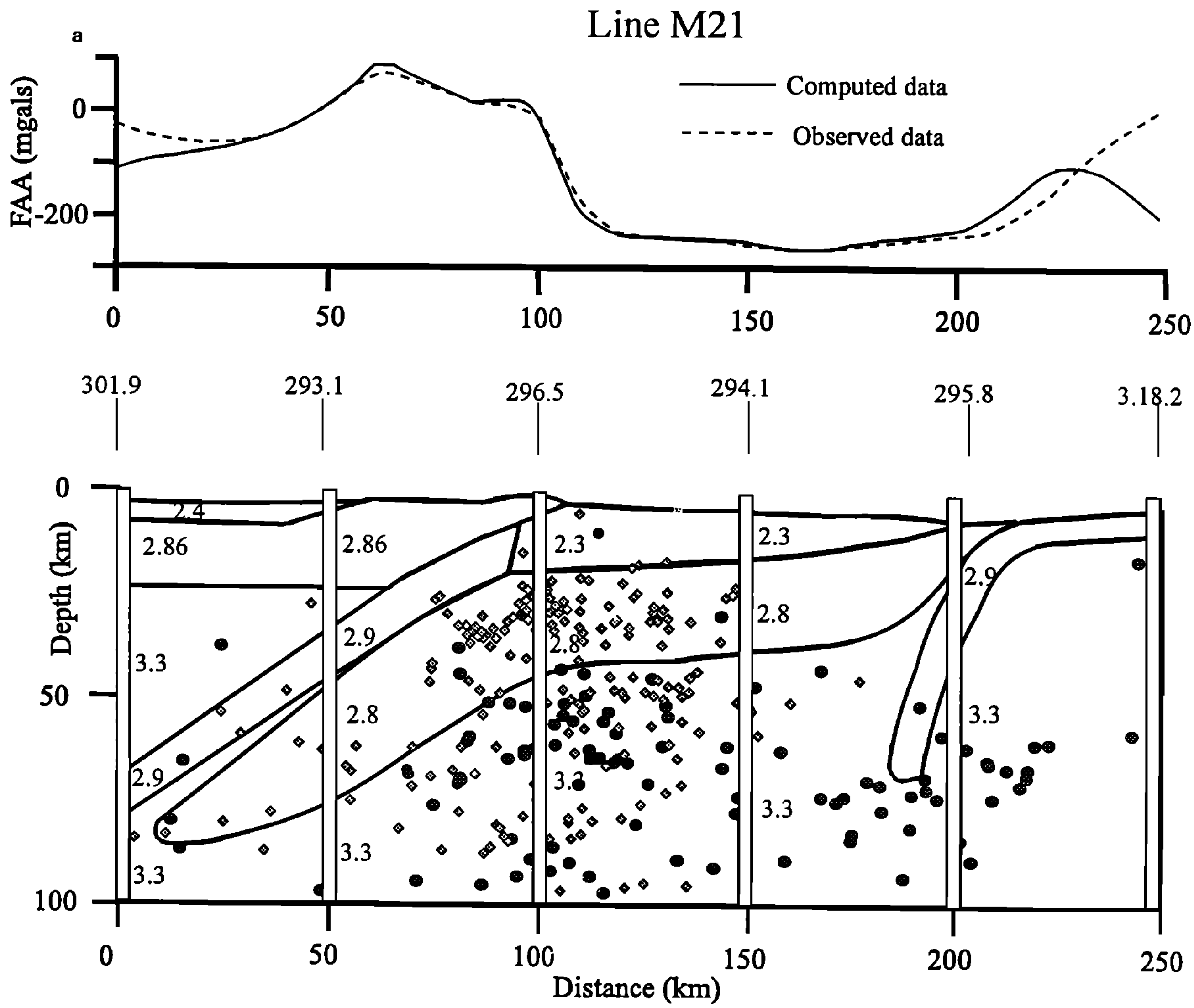

Figure 9. .Two-dimensional gravity modeling for (a) line M21 and (b) lineM31 (locations in Figure 1 and 4). Digits inside the polygons are the chosen densities. Observe the rupture of the crust beneath the accretionary wedge and the underplatting of the Snellius Ridge beneath the long west dipping Molucca slab. Diamonds indicate the seismicity recorded by the OBS network during the MODEC cruise. Circles indicate the global seismicity. Mass columns are in kg/cm^2.

4.2. Two-Dimensional Modeling

We have computed the FAA of the MODEC cruise along several east-west profiles. Bathymetric data included in the modeling correspond to the vertical beam of the echo sounder.

On the basis of our bathymetric and seismic observations, we have tested models consistent with a simple subduction system composed of a forearc basin (the Sangihe Basin), an ophiolitic backstop (the Molucca Ridge), which induces a strong and narrow positive gravity anomaly, and a thick accretionary wedge with low densities, underlined by a strong negative anomaly. Having no seismic refraction data, we have used the depth of earthquakes to constrain the models. Unfortunately, the data east of Talaud island are too scarce to allow any modeling at this very latitude. Thus the observed gravity is extracted from the lines M21 and M31 of the MODEC cruise (Figure 9, location in Figures 1 and 4), northeast of Talaud. These profiles do not intersect a wide part of the Snellius Ridge, but line M31 passed over the northern narrow end of the plateau (Figure 1). Line M21 intersects the gravity low of the accretionary wedge.

From the Sangihe arc to the accretionary wedge, the two profiles computed (Figure 9) show a decrease of approximately 400 mGal. The sections of the gravity profiles located above the Pujada-Miangas Ridge show a double peak. On line M21 these two peaks correspond to the Miangas and Pujada Ridges separated by the central depression. Southward, the Pujada Ridge is not visible in the bathymetry, but its gravity signature extends south of the latitude 5°N (line M31, Figure 9b). North of line M21, the two ridges merge, and the gravity signature of the Pujada-Miangas Ridge becomes a single broader anomaly. In

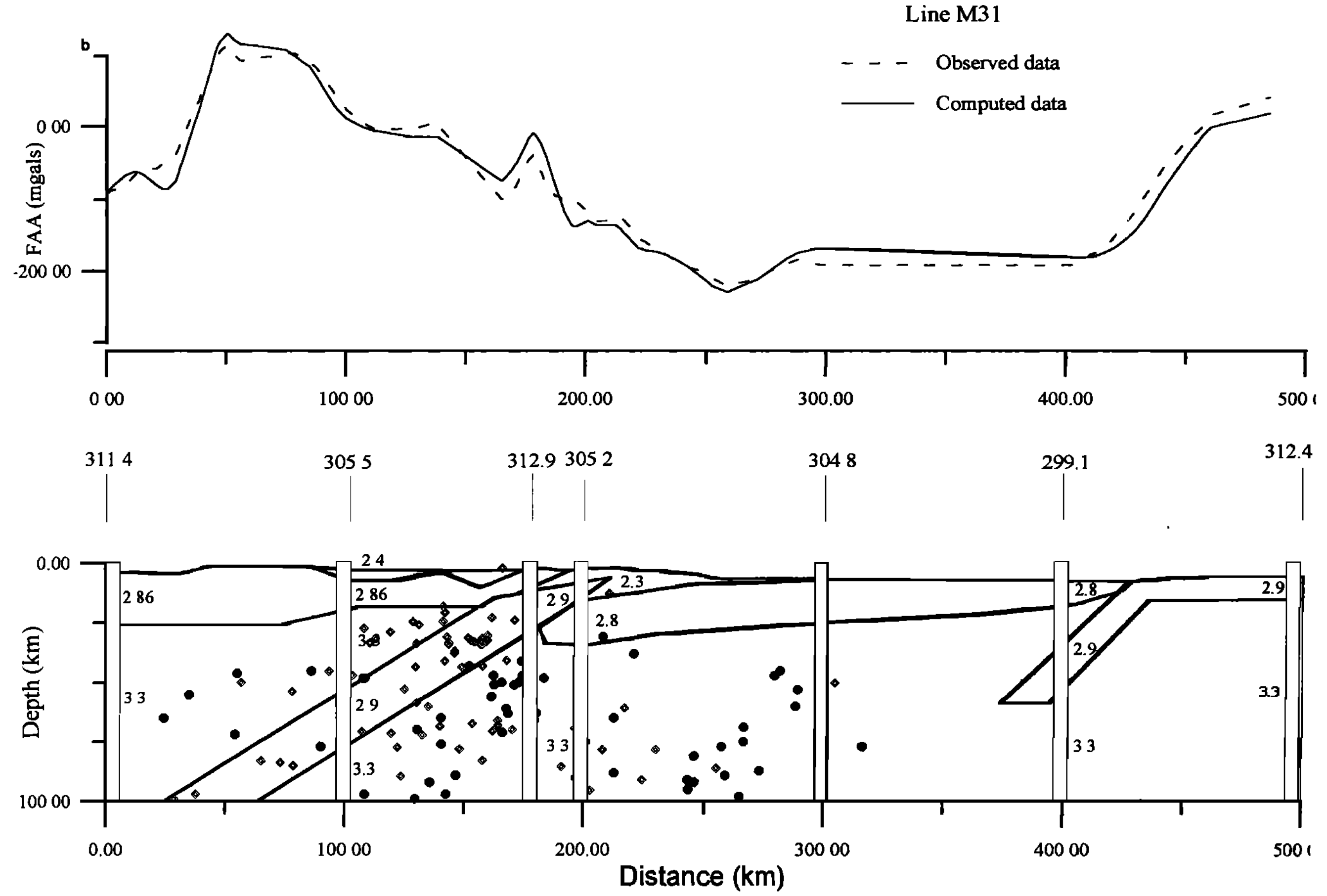

Figure 9. (Continued)

order to cope with the strong negative anomaly of the wedge, we modeled several geometries and densities for line M21 until we got the best fit. For the following profile (line M31) these parameters were applied, without additional testing.

The first step was to compute the gravity response for a simple thick and light accretionary wedge underthrusted by an oceanic slab dipping to the west at low angle. Several geometries for the slab were tested, with wedge densities ranging from 1.8 to 2.2 for each (Figure 10).

In order to cope with the measured values, we tried densities lower than 1.9. The negative anomaly computed with such densities is too low at the foot of the ridge and increases rapidly when the slab reaches the surface. Furthermore, these values do not seem reasonable, even for uncompacted sediments. Then we explored densities of 2.1 or 2.2, values used for classical subduction complexes [*Lallemant et al.*, 1989]. With such values, the large-wavelength anomaly can be modeled, but on the other hand, the gravity minimum induced by such a wedge is too weak to fit the observed data (down to -300 mGal at 6°05'N).

We also tried unsuccessfully to tilt the basement roof, meaning an increase of the subduction angle, keeping it within a range suitable with the seismic data (not illustrated). However, such geometry did not respect the thickness of the wedge at the foot of the ridge and created a greater sagging of the simulated curve.

Because a basement deepening seems to be the only alternative, we finally considered a basement rupture within the undergoing plate. This model deepens the basement without changing the angle of the subduction (Figures 9a and b).

Such models (Figures 9a and b) fit well both sides of the trench on line M21, and the computed gravity anomaly reaches the negative values of the wedge with a density of 2.3 for the sediments. Line M31 shows a good fit for the section overlain by the wedge. As for line M21 (see above, Figure 9a), a basement rupture helps to explain the steep gradient located above the eastern side of the Miangas Ridge.

Such rupture in the downgoing plate is supported by the results of the two OBS networks deployed during the MODEC cruise. OBS were extremely useful for improving our knowledge of the seismic activity, 3 weeks recording by the OBS, having produced more data than years of global seismicity. On the northern network (located around the Miangas island), dense seismic activity occurred from the surface to 100 km depth. In addition, the velocity model deduced from relocation of microseismicity indicates that the crust thickness reaches 60 km minimum beneath the Molucca Ridge. These data helped us to constrain the density used for gravity modeling.

Our model suggests that the downgoing slab is broken just below the ophiolitic ridge. Presence of seismicity demonstrates that this process is active. The uplift of the broken slab can be facilitated by the subduction of the buoyant Snellius Ridge, which is forced into the trench and thrusted under the Molucca slab (line M21). Strong coupling into the subduction zone induced the deformation of the forearc region, like backthrusting of the outer ridge (Talaud pop-up structure) and thrusting and

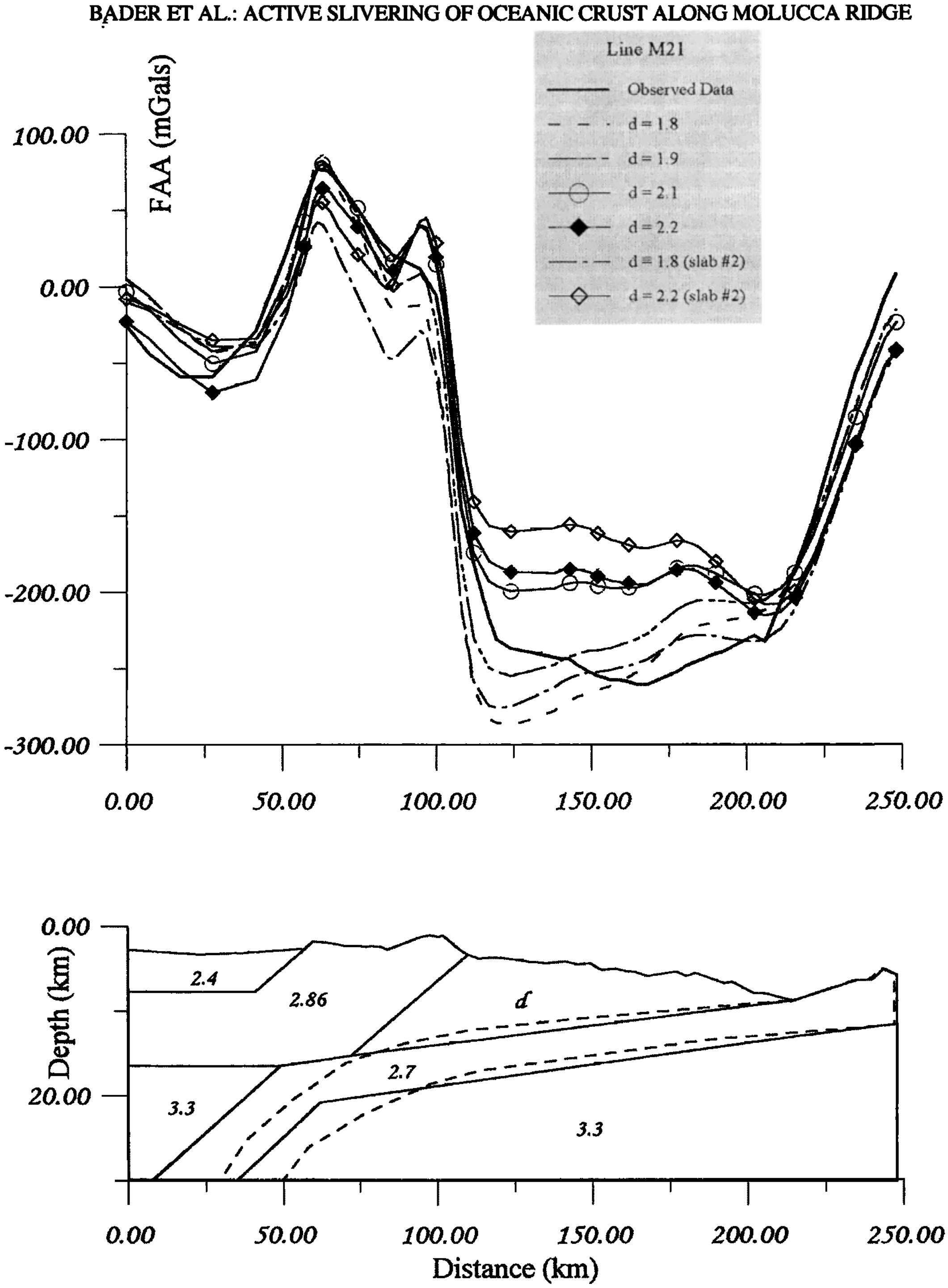

Figure 10. Two-dimensional model and graph on line M21 (location in Figure 1 and 4) with varying wedge densities from d=1.8 to d=2.2 and observed gravity (bold line). With two simple slab geometries and bending, none of the densities fit the amplitude or the shape of the observed curve.

folding in the forearc basin. The nascent Philippine Trench could also be a consequence of this strong coupling.

5. Discussion

In the northern Molucca Sea the broken oceanic crust is underthrusted actively beneath the Molucca Ridge (Miangas and Talaud Ridges). Nevertheless, the ridge was deformed and uplifted before the middle Miocene. The large time gap between these two periods of oceanic crust deformation may be interpreted in two different ways:

1. Within a unique tectonic process, incorporation of the ophiolites into the wedge could be regarded as an occasional event, most of the oceanic material between the present and the Middle Miocene having been subsequently subducted into the mantle.

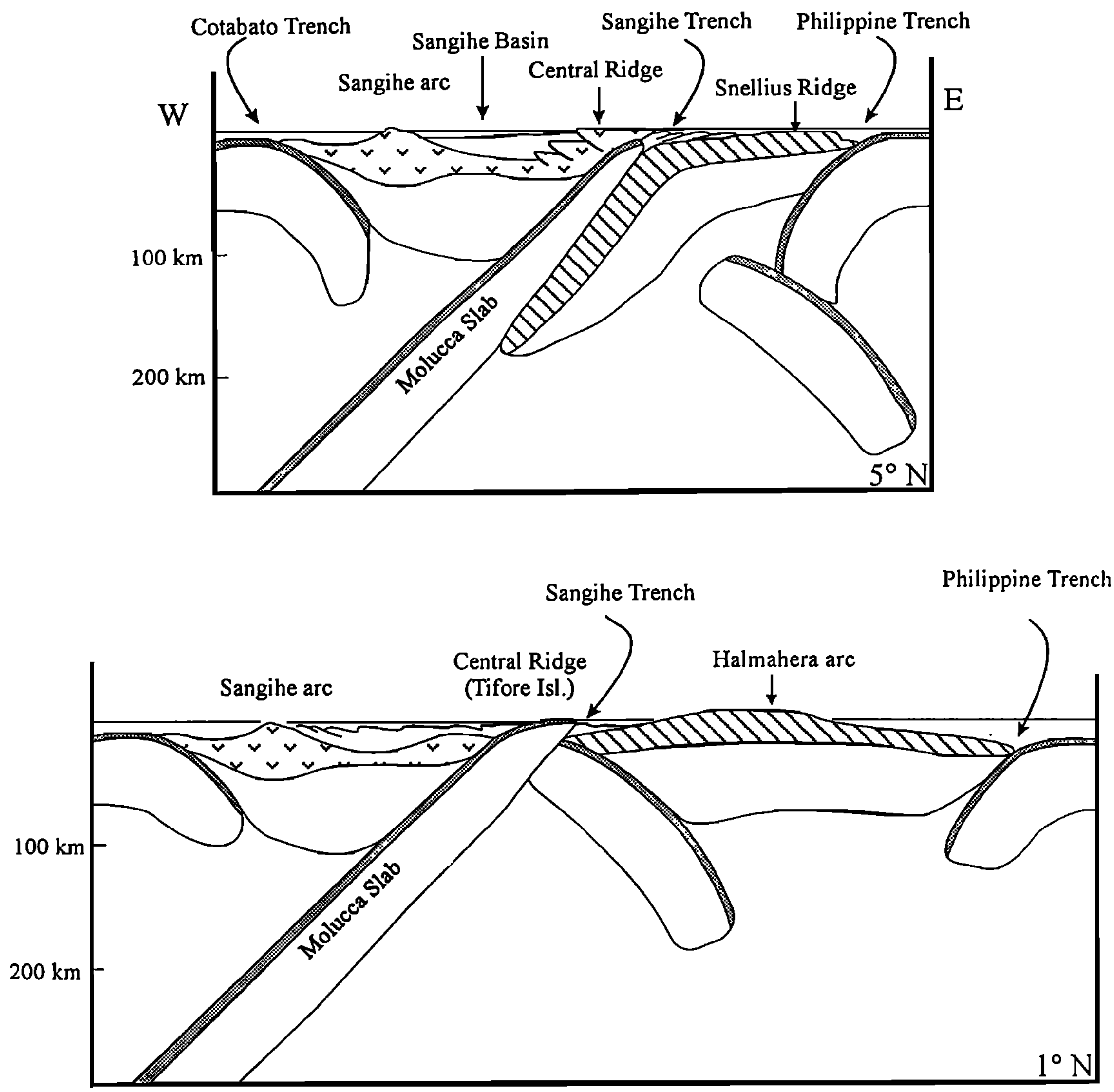

Figure 11. Interpretative cross section showing the subduction of the Snellius Ridge beneath the Eurasian margin at (top) 5° N, the Snellius ridge is forced in the subduction. The forearc is backthrusted and emerge and at 1° N (bottom), the double Molucca slab is ruptured at the top and the Philippine trench is initiated.

2. In contrast, the formation of the ophiolitic Molucca Ridge may be independent of the active deformation of the Molucca lithosphere. In this case its rupture would happen only during the final stage of subduction, and we may consider that the broken Molucca slab still undergoes continuous subduction like any other oceanic asperity. Such a subduction of slivered oceanic crust was discussed by *Lallemant et al.* [1989] in the Nankai Trough where the Shikoku basin oceanic crust was deformed and slivered along the Zenisu Ridge before it got subducted in the Nankai Trough. In this case another geodynamic scenario has to be proposed for the deformation and uplift of the Molucca Ridge.

The onset of subduction along the Sangihe arc could have been developed in the center of a large oceanic basin extending from the Celebes Sea to the Molucca Sea and even extending to the west Philippine Basin according to *Hall* [1996]. The Sangihe arc was built on this basin, the remnant of which is now exposed in the Sangihe outer ridge (the Molucca ridge). The Eocene age of the Talaud ophiolites [*Evans et al.*, 1983] and the Celebes Sea oceanic floor [*Weissel*, 1980] are in agreement with this idea.

Two distinct tectonic scenarios must be invoked for the origin of the Molucca Ridge ophiolites and the ruptured oceanic slab. Both could be part of the same oceanic basin but do not represent the same event. The outer ridge ophiolite is coeval with the onset of subduction along the Sangihe forearc whereas the ruptured oceanic crust results from the last stage of subduction along the Sangihe trench system. The age of the beginning of the Sangihe subduction is given by the age of the oldest volcanic rocks sampled all along the Sangihe arc, the age of the tephras in the neighboring basins, and the age of the oldest sediments deposited in the forearc. The Awit Formation described in the Talaud islands and bearing abundant tuffaceous sediments [*Sukamto and Suwarna*, 1986] may record the beginning of explosive arc activity by the middle Miocene. It is unconformably overlying older rocks which are more deformed and therefore marking a pre-middle-Miocene tectonic event. At the latitude of Talaud, Ocean Drilling Program (ODP) leg 124 located in the Celebes Sea also drilled a section with numerous occurrences of tephras dated from 8 Ma at 410 mbsf [*Pubellier et al.*, 1991b]. Rocks dated around 10 Ma have been found in Sarangani Peninsula [*Pubellier et al.*, 1991a; *Bellon and Rangin*, 1991] within a volcaniclastic series overlying middle Miocene limestone. It is then possible that the Sangihe arc was formed at approximately 15 Ma.

Other ophiolites were also emplaced around 15 Ma in Taiwan [*Pelletier and Stephan*, 1986] and in Mindoro [*Rangin et al.*, 1985]. The onset of the Sangihe trench may be included into a wider scale change in the motion of the Philippine Sea plate around 15 Ma (X. Le Pichon, La déformation du Japon, cours du Collège de France, 1997).

As a conclusion, it is clear that the structure of the central part of the Molucca Sea emphasizes several stages of oceanic crust deformation. An early stage of slivering for an Eocene oceanic basin is marked by thrusting and emplacement of ophiolites in Talaud islands (Kabaruang ultramafics). We do not have enough geological information to reconstruct precisely the geodynamic setting of the area in early middle Miocene key period, but we can reasonably infer that the ophiolites of the outer ridge have been deformed and incorporated into the Sangihe forearc a long time before the present deformation of the Molucca Sea slab at depth.

From the middle Miocene to the present, the Molucca Sea lithosphere subducted under the Sangihe arc. This subduction was first perturbated by the rupture of the "U-shaped" Molucca Sea lithosphere (Figure 11, bottom) and then by the penetration of the Snellius Ridge under the west dipping Molucca slab (Figure 11, top).

Acknowledgments. This work was possible due to the co-operation programs between France, the Philippines, and Indonesia. We want to thank particularly E. Domingo in the Bureau of Mines and Geosciences in Manila and D. Zen of BPPT in Djakarta. DTM was computed by B. Deffontaines (CNRS-UPMC). Some modeling parameters were taken from C. Widiwijayanti. Laboratory facilities were supplied by the Université. P. et M. Curie and Ecole Normale Supérieure in Paris We thank E.R. Flüh and C. Bowin for constructive reviews of the manuscripts. Three of the authors (M.P, C.R., and C.D.) belong to the Centre National de la Recherche Scientifique (CNRS).

References

Bellon, H., and C. Rangin, Geochemistry and isotopic dating of Cenozoic volcanic arc sequences around the Celebes and Sulu seas, *Proc. Ocean Drill Program Sci. Results, 124*, 321-338, 1991.

Evans, C. A., J. W. Hawkins, and J. F. Moore, Petrology and geochemistry of ophiolitic and associated volcanic rocks on the Talaud island, Molucca Sea collision zone, northeast Indonesia, in *Geodynamics of the Western Pacific-Indonesian Region, Geodyn. Ser.*, vol. 11, edited by T.W.C. Hilde and S. Uyeda, 159-172, AGU, Washington, D.C, 1983.

Hall, R., Reconstructing Cenozoic SE Asia, in *Tectonic Evolution of Southeast Asia*, edited by R. Hall and D Blundell, Geol. Soc. Spec. Publ., *106*, 153-184, 1996.

Hall, R., G. Nichols, P. Ballantyne, T. Charlton, and J. Ali, The character and significance of basement rocks of the southern Molucca Sea region, *J. of Southeast Asian Earth Sci*, *6* (3/4), 249-258, 1991.

Hall, R., J. R. Ali, and C. D. Anderson, Cenozoic motion of the Philippine sea plate: Palaeomagnetic evidence from eastern Indonesia, *Tectonics*, *14* (5), 1117-1132, 1995.

Hamilton, W., Tectonics of the Indonesian region, *U.S. Geol. Surv. Prof. Pap.*, *1078*, 1708 pp 1979.

Hawkins, J. W, G. F Moore, R. Villamor, C. Evans, and E. Wright, Geology of the composite terranes of East and Central Mindanao, *Tectonostratigraphic Terranes of the Circum Pacific Region*, edited by D.G. Howell, pp. 437-463, AGU, Washington, D.C., 1985.

Huang, S., I.S. Sacks, and J A. Snoke, Topography and seismic effects of long-term coupling between the subduction and overriding plates beneath Northeast Japan, *Tectonophysics*, *269*, 279-297, 1997.

Krause, D.C., Tectonic, marine geology and bathymetry of the Celebes-Sulu sea region, *Geol Soc. Am. Bull.*, *77*, 813-831, 1966

Lallemant, S., N. Chamot-Rooke, X. Le Pichon, and C. Rangin, Zenisu ridge: A deep intraoceanic thrust related to subduction, off Southwest Japan, *Tectonophysics*, *160*, 151-174, 1989.

McCaffrey, R., Lithospheric deformation within the Molucca Sea arc-arc collision: Evidence from shallow and intermediate earthquake activity, *J. Geophys. Res.*, *87*, 3663-3678, 1982.

McCaffrey, R, Earthquakes and ophiolite emplacement in the Molucca Sea collision zone, Indonesia, *Tectonics*, *10* (2), 433-453, 1991.

McCaffrey, R., E A. Silver, and R. W. Raitt, Crustal structure of the Molucca Sea collision zone, Indonesia, *The Tectonic and Geologic Evolution of Southeast Asian Seas and Islands, Geophys. Monogr. Ser*, vol. 23, edited by D.E. Hayes, pp. 161-177, AGU, Washington, D.C, 1980

Moore, G F., D Kadarisman, and R. Sukamto, New data on the geology of the Talaud islands, Molucca sea, *Geol. Res. Dev. Cent. Bull.*, *3*, 5-12, 1980.

Nichols, G. H, R. Hall, J Milsom, and D. Masson, The southern termination of the Philippine trench, *Tectonophysics*, *183*, 289-303, 1990.

Pelletier, B. and J F. Stephan, Middle Miocene obduction and late Miocene beginning of collision registered in the Hengchun Peninsula: Geodynamic implications for the evolution of Taiwan, *Tectonophysics*, *125*, 133-160, 1986.

Pubellier, M., R. Quebral, C. Rangin, B. Deffontaines, C. Muller, J. Butterlin, and J Manzano, The Mindanao collision zone: A soft collision event within a continuous Neogene strike-slip setting, *J Southeast Asian Earth Sci.*, *6* (3/4), 239-248, 1991a.

Pubellier, M, P Spadea, A. Pouclet, R Solidum, A. Desprairies, and H Cambray, Correlations on tephras in Celebes and Sulu Sea Basin : Constraints on geodynamics, *Proc. Ocean Drill. Program Sci. Results*, *124*, 459-465, 1991b.

Pubellier, M., R. Quebral, M Aurelio, and C. Rangin, Docking and post-docking escape tectonics in the southern Philippines, in *Tectonic Evolution of Southeast Asia*, edited by R Hall and D. Blundell, *Geol. Soc. Spec. Publ*, *106*, 511-523, 1996.

Quebral, R., M. Pubellier, and C. Rangin, The onset of movement on the Philippine Fault in eastern Mindanao: A transition from a collision to a strike-slip environment, *Tectonics*, *15* (4), 713-726, 1996.

Rangin, C., J. F. Stephan, and C. Muller, Middle Oligocene oceanic crust of South China Sea jammed into Mindoro collision zone (Philippines), *Geology*, *13* (6), 425-428, 1985.

Rangin, C et al, Collision and strike slip faulting in the northern Molucca sea (Philippines Indonesia): Preliminary results of a morphotectonic study, in *Tectonic Evolution of Southeast Asia*, edited by R. Hall and D Blundell, *Geol. Soc. Spec. Publ.*, *106*, 29-46, 1996.

Silver, E. A., and J. C. Moore, The Molucca sea collision zone, Indonesia, *J. Geophys. Res.*, *83*, 1681-1691, 1978.

Silver, E. A., and J. C. Moore, The Molucca sea collision zone, Indonesia, in *The Geology and Tectonics of Eastern Indonesia*, edited by A.J. Barber and S. Wiryosujono, *Geol. Res. Dev. Cent. Spec. Publ.*, *2*, 327-340, 1981.

Smith, W. H F, and D. T. Sandwell, Marine gravity field from declassified Geosat and ERS-1 altimetry, *Eos Trans AGU*, *76* (46), Fall Meet. Suppl., F156, 1995.

Sukamto, R, and N. Suwarna, The geology of the Talaud quadrangle, North Sulawesi, geological map, Geol. Res and Dev. Centre, Bandung, 1986.

Weissel, J.K., Evidence for Eocene oceanic crust in the Celebes basin, in *The Tectonic and Geologic Evolution of Southeast Asian Seas and Islands, Geophys. Monog. Ser.*, vol. 23, edited by D.E. Hayes, pp. 37-47, AGU, Washington, D.C, 1980.

A. G. Bader, Institut Français du Pétrole, 1 & 4 Av. de Bois Préau, 92852 Rueil Mailmaison Cedex, France (gaelle.bader@ifp.fr)

C. Deplus and R Louat, Laboratoire de gravimétrie et géodynamique, Institut de Physique du Globe, T26-16 E3, 4 Pl. Jussieu, 75252 Paris, France.

M. Pubellier and C. Rangin, Laboratoire de géologie de l'ENS, URA 1316 CNRS, 24 rue Lhomond, 75005 Paris.

(Received February 14, 1997;
revised August 19, 1998;
accepted August 30, 1998.)